Am J Cancer Res 2024;14(1):73-85
www.ajcr.us /ISSN:2156-6976/ajcr0152428

Original Article

Nomograms for predicting clinically significant prostate cancer in men with PI-RADS-3 biparametric magnetic resonance imaging

Zhen Liang[1*], Tianrui Feng[1*], Yi Zhou[1], Yongjiao Yang[2], Yujiao Sun[1], Zhien Zhou[1], Weigang Yan[1], Fenghong Cao[3]

[1]*Department of Urology, Peking Union Medical College Hospital, Peking Union Medical College, Chinese Academy of Medical Sciences, Beijing, China;* [2]*Department of Urology, The Second Hospital of Tianjin Medical University, Tianjin Medical University, Tianjin, China;* [3]*Department of Urology, North China University of Science and Technology Affiliated Hospital, No. 73 Jianshe South Road, Tangshan, Hebei, China.* [*]*Equal contributors.*

Received July 25, 2023; Accepted December 4, 2023; Epub January 15, 2024; Published January 30, 2024

Abstract: This study aimed to construct nomograms for predicting the likelihood of clinically significant prostate cancer (csPCa) in patients with lesions rated as Prostate Imaging Reporting and Data System (PI-RADS) 3 on biparametric magnetic resonance imaging (bpMRI). We retrospectively analyzed a cohort of 457 patients from the Peking Union Medical College Hospital (January 2017-July 2021) to develop the model and externally validated it with a cohort of 238 patients from the Second Hospital of Tianjin Medical University (September 2017-September 2021). Univariate and multivariate logistic regression analyses identified significant predictors of csPCa, defined by tumor volumes ≥ 0.5 cm^3, Gleason score ≥ 7, or presence of extracapsular extension. Diagnostic performance for the peripheral zone (PZ) and transitional zone (TZ) was compared using the receiver operating characteristic (ROC) curve and decision curve analysis (DCA). Through univariate and multivariate logistic regression analyses, we identified age, prostate-specific antigen (PSA), and prostate volume (PV) as predictors of csPCa for the PZ, and age, serum-free to total PSA ratio (f/t PSA), and PSA density (PSAD) for the TZ. The nomograms demonstrated robust discriminative ability, with an area under the ROC curve (AUC) of 0.819 for PZ and 0.804 for TZ. The external validation corroborated the model's high predictive accuracy (AUC of 0.831 for PZ and 0.773 for TZ). Calibration curves indicated excellent agreement between predicted and observed outcomes, and DCA underscored the nomogram's clinical utility for both PZ and TZ. Overall, the nomograms offer high predictive accuracy for csPCa at initial biopsy, potentially reducing unnecessary biopsies in clinical settings.

Keywords: Prostatic neoplasms, magnetic resonance imaging, prostate biopsy, nomogram, predictive model

Introduction

Prostate cancer (PCa) is one of the most common malignancies in men globally and its incidence is expected to increase in the coming decades [1, 2]. The serum prostate-specific antigen (PSA) test is widely applied both in detection and monitoring for PCa. However, multiple previous studies indicate limited cancer detection rates of 11.8-20.5% for PSA levels of 4-10 ng/mL, and 20.5-25.0% for 10-20 ng/mL [3, 4]. The low specificity of PSA levels and detection of clinically insignificant PCa (insPCa) has been noted, resulting in overdiagnosis and subsequent overtreatment without improving overall survival [5]. Multiparametric magnetic resonance imaging (mpMRI), comprising T2-weighted imaging (T2WI), Diffusion-weighted imaging (DWI), and Dynamic Contrast Enhancement (DCE), has emerged as a valuable tool in prostate biopsy decision-making [6]. Generally, DCE is especially applied to upgrade Prostate Imaging Reporting and Data System (PI-RADS) 3 lesions located in the peripheral zone (PZ) to PI-RADS 4 if DCE enhancement is positive. Although DCE could be helpful in particular cases, its requirement for intravenous gadolinium as contrast media leads to an increased risk of gadolinium accumulation in numerous organs including the

https://doi.org/10.62347/XBBI9870

brain, renal glomeruli, and bones with possible clinical sequelae [7, 8]. Biparametric MRI (bpMRI), which consists of T2WI and DWI, is increasingly being applied for the detection and characterization of PCa [9]. Compared with mpMRI, bpMRI is quicker (~15 minutes) and simpler, while sufficiently retaining the diagnostic accuracy [10]. However, the exclusion of DCE in mpMRI may increase PI-RADS 3 scored lesions due to the role of DCE in the diagnosis of PI-RADS 3 lesions, though previous studies have reported that the positive rate of clinically significant prostate cancer (csPCa) in PI-RADS 3 lesions is not high [11]. Therefore, what is the best method for patients with a PI-RADS 3 to avoid unnecessary prostate biopsies without compromising the detection of csPCa remains controversial.

This study aims to develop nomograms based on bpMRI for predicting initial prostate biopsy outcomes in patients with PI-RADS 3 lesions, potentially replacing DCE in the PI-RADS scoring system. Given that DCE is a secondary sequence in PI-RADSv2.1, mainly for characterizing PZ lesions [12], we developed separate nomograms for the PZ and transition zone (TZ). These predictive nomograms could assist urologists in determining the necessity of biopsies for patients with indeterminate bpMRI results. Multiple predictive models based on bpMRI findings and clinical parameters for csPC risk assessment have recently been reported [9, 13, 14], nevertheless, there is still scope for improvement. Considering that most of prediction models have not been applied clinically, we performed our research under the guidance of TRIPOD (transparent reporting of multivariate prediction models for individual prognosis or diagnosis) for multivariate prediction models (http://www.tripod-statement.org) [15].

Materials and method

Patient selection

The training cohort was consecutively selected from patients who underwent initial cognitive MRI targeted biopsy combined with transrectal ultrasound-guided (TRUS) transperineal systematic prostate biopsy in the urology department of Peking Union Medical College Hospital from January 2017 to July 2021. The prostate biopsy was performed through an automatic biopsy gun with an 18-gauge needle under TRUS guidance. Patients were placed in the lithotomy position. The surgeon reviewed the MRI images and the report before the biopsy. Systematic biopsy was performed following the Ginsburg protocol with at least 12 cores [17]. Additional two or three targeted biopsies were acquired from suspected areas detected on MRI. Index lesions were used to represent the malignancy of the tumor for the final analyses and defined as the largest or the highest Gleason score tumor-bearing lesion. The Gleason score was determined on biopsies specimen by pathologists specialized in urology and the csPCa was defined as PCa with tumor volumes ≥ 0.5 cm^3 or Gleason score ≥ 7 or extracapsular extension [18].

Biopsy indications included: (1) total serum PSA > 10.0 ng/ml; (2) total serum PSA between 4.0 and 10.0 ng/ml with a free to total PSA ratio (f/t PSA) < 0.16 or a PSA density (PSAD) > 0.15; (3) abnormal digital rectal examination (DRE); and (4) suspicious findings on TRUS or mpMRI. A set of exclusion criteria was formulated for screening the eligible patients in both centers. (1) Only the prostate naive biopsy was considered in this study. (2) The enrolled cases must have complete baseline clinicopathologic information; patients with any missing value were discarded. (3) Patients with a history of other malignancies or a family history of PCa were excluded. (4) Patients with extreme total serum PSA values (PSA > 20 ng/ml or PSA < 4 ng/ml) were eliminated because in the initial biopsy setting, when PSA > 20 ng/mL, the role of nomogram is less useful since patients should be submitted to a biopsy regardless of other parameters.

To conduct TRIPOD validation, it is necessary to externally validate data from different locations or times. For this purpose, an external validation cohort was recruited from the urology department, Second Hospital of Tianjin Medical University from September 2017 to September 2021. The inclusion and exclusion criteria of the validation cohort were consistent with the training cohort. The patient selection flow chart is demonstrated in **Figure 1**. Written informed consent was obtained from all participants in terms of the storage of their information for research.

Data extraction

All data were analyzed anonymously during the process. This retrospective study was

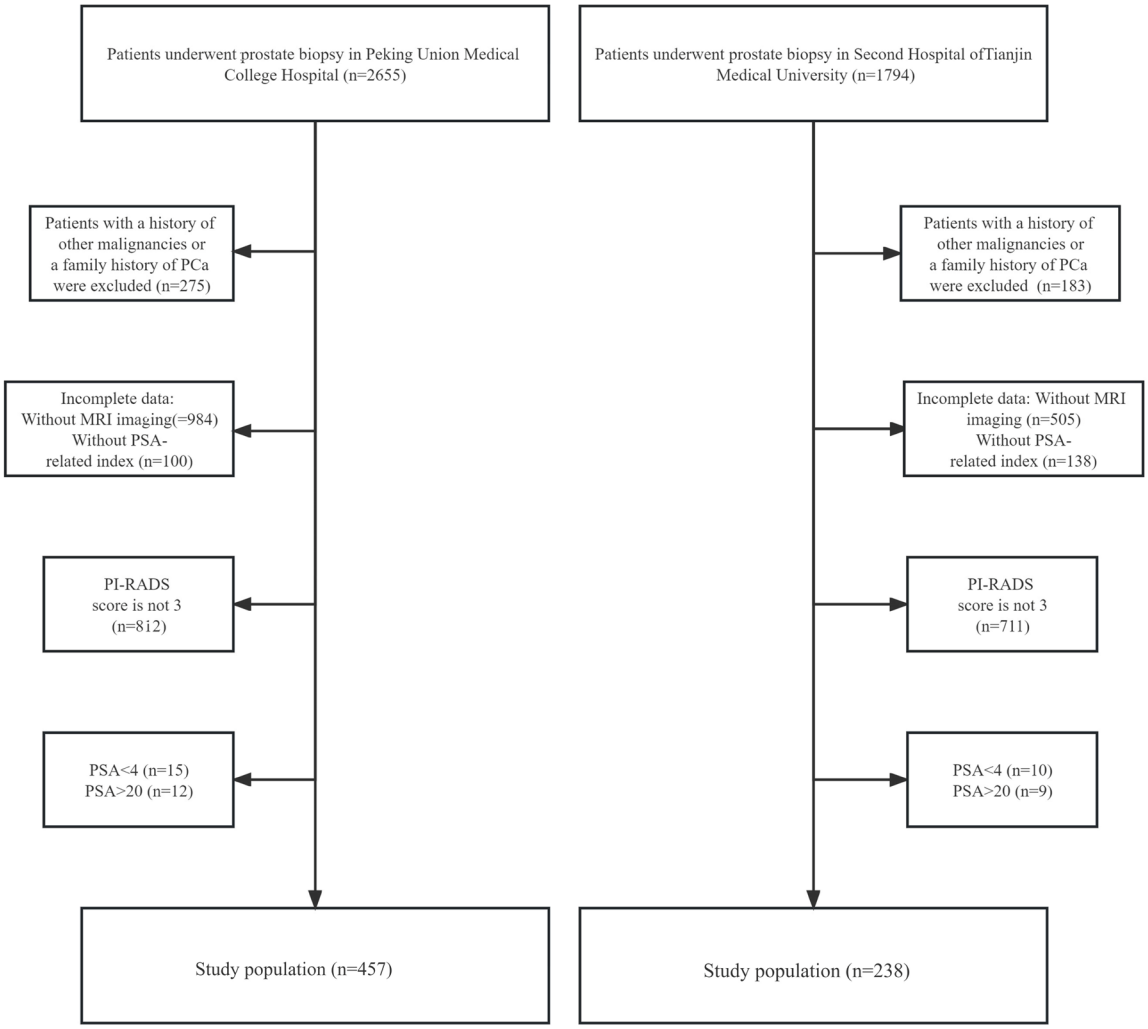

Figure 1. Patient selection flow chart.

performed in compliance with the guidance of the Declaration of Helsinki. Serum PSA and f/t PSA levels were obtained pre-biopsy along with DRE. Prostate volume (PV) was calculated as anteroposterior diameter × vertical diameter × transverse diameter × 0.52 according to MRI. PSAD was calculated by dividing the PSA by the PV. Since PSAD was made up of PSA and PV, PSAD cannot be analyzed together with the combination of PSA and PV for multivariate logistic regression analyses, thus warranting separate analyses and the more significant one was chosen.

The Institutional Review Boards of both Peking Union Medical College and Tianjin Medical University approved the study.

Outcome measures

Two genitourinary radiologists, each with over five years of specialization, independently reported all MRI readings, blind to clinical data, diagnosis, and pathology (Z.Y. and Z.Z.). The radiologists read the images twice following the PI-RADS v2.1 in two different sessions. During the first reading session, the radiologists read mpMRI (T2WI, DWI, ADC map, and DCE imaging) to determine the PI-RADS categories. After initial readings and a four-week interval, the same radiologists reassessed each image using bpMRI comprising T2WI in three planes and DWI to determine the PI-RADS categories derived from the index lesion according to a modified PI-RADS v2.1

(Supplementary Table 1). The inter-reader agreement was assessed through Cohen's kappa analysis. The kappa (κ) value was interpreted as suggested: κ < 0.20 (poor agreement), κ=0.21-0.40 (fair agreement), 0.41-0.60 (moderate agreement), 0.61-0.80 (high agreement), and 0.81-1.00 (very high agreement) [16]. Disagreements were resolved through consultation with a senior genitourinary radiologist with more than 20 years of experience (Y.W.). The detailed MRI acquisition parameters are displayed in Supplementary Table 2. ADC maps were automatically generated through voxelwise calculation. The targeted lesions were marked on T2WI for the following cognitive biopsy. According to MRI results, the prostate was divided into four parts: left PZ, left TZ, right PZ and, right TZ. Lesions spanning two adjacent regions were considered a single lesion for the purposes of this study.

Statistical methods

We characterized the distribution of baseline patient demographics and clinical variables using the median and interquartile range (IQR), appropriate for skewed data distributions. CsPCa detection rates of PZ and TZ were compared using the chi-square test. Univariate regression analysis was initially used among age, PSA, f/t PSA, PSAD, PV, DRE, lesion size and quantity based on bpMRI to evaluate the difference between the csPCa group and insPCa group, and identified significant risk factors for the subsequent multivariate logistic regression analysis, upon which a predictive nomogram would be established. The performance of the nomogram was quantified using odds ratios (ORs), 95% confidence intervals (CIs), and *p*-values, with the area under the curve (AUC) assessing discrimination capability.

Model reliability was enhanced through bootstrap resampling (1000 replicates) to calculate 95% CIs for the nomogram's predicted probabilities. All analyses were conducted using R software version 4.1.2 (The R Foundation), with a significance threshold set at P < 0.05. Key packages implemented included 'survival' (3.5-5), 'rms' (6.7-0), and 'timeROC' (0.4) (http://www.r-project.org/). The clinical utility of the nomogram was further evaluated using decision curve analysis (DCA) [19], and the Hosmer-Lemeshow test alongside calibration plots were used to assess the concordance between predicted and actual outcomes.

External validation of the nomogram encompassed analyses of discrimination, calibration, and DCA. Receiver operating characteristic (ROC) curves were generated, and the DeLong test was utilized to compare AUC values between the training and validation cohorts, ascertaining the model's discriminative capacity and potential overfitting. Calibration curves plotted predicted versus observed probabilities to appraise predictive accuracy, with an ideal model demonstrating a calibration curve that closely approximates the 45-degree line, denoting perfect prediction. DCA was applied to evaluate the net benefit of the developed models.

Results

Patient characteristics

Table 1 presents the clinical and pathological characteristics of 457 patients comprising our training cohort. Of these, 258 (56.4%) had a negative biopsy, and 199 (43.6%) were diagnosed with PCa, with 140 (70.4%) classified as csPCa and 59 (29.6%) as indolent PCa. Despite the presence of DCE positive findings in 156 patients, the csPCa rates did not significantly differ between DCE-negative (29.5%) and DCE-positive (32.6%) patients (P=0.521). A shift from PI-RADS 3 to PI-RADS 4 was observed in 97 patients with PZ lesions due to positive DCE, of whom 21 were diagnosed with csPCa. The nomogram, alongside bpMRI, recommended biopsies for 20 of these patients due to a high csPCa probability. The inter-reader reliability for PI-RADS scoring between two radiologists was in "very high agreement" level (kappa: 0.83, 95% CI: 0.75-0.92, P=0.002). The median age of the study participants was 65 years (IQR, 61-71), with a median serum PSA level of 7.64 ng/mL (IQR, 5.72-10.64) and a median PV level of 45 mL (IQR, 34-60). The median values of PSAD and f/t PSA were 0.173 ng/mL (IQR, 0.088-0.254) and 0.154 (IQR, 0.078-0.134), respectively. A total of 457 PI-RADS 3 index lesions were detected according to bpMRI. Based on our results, PI-RADS 3 index lesions were more frequently located in the TZ (n=245) than in the PZ (n=212), yet the csPCa detection rate was significantly higher in the PZ (45.2%, 96/212) compared to the TZ (17.9%, 44/245)

Table 1. Baseline characteristics of included patients for internal validation

Variables	insPCa		csPCa	P
	Non-PCa	indolent PCa		
Patients n	258	59	140	
Age (median)	64 (60-70)	65 (62-72)	70 (65-76)	< 0.001
PSA (median)	6.52 (5.55-10.35)	7.10 (5.90-11.1)	11.83 (8.00-22.70)	< 0.001
f/tPSA (median)	0.151 (0.144-0.212)	0.133 (0.090-0.199)	0.114 (0.083-0.160)	0.035
PV (median)	45 (35-60)	35 (30-50)	35 (30-45)	< 0.001
PSAD (median)	0.149 (0.100-0.247)	0.202 (0.150-0.286)	0.342 (0.218-0.633)	0.003
T stage				< 0.001
T2a		31 (52.2%)	53 (38.2%)	< 0.001
T2b		3 (5.1%)	22 (15.8%)	< 0.001
T2c		25 (42.7%)	65 (46.4%)	< 0.001
Percentage cores positive		7.20% (547/7592)	6.11% (464/7592)	
Lesion size (median, mm)		7.5 (6-11)	7 (5-11)	0.417
Lesion quantity (average)		1.12	1.26	0.518

Table 2. Multivariate regression for the detection of clinically significant cancer on initial prostate biopsy

Variables	Multivariable model		
	Adjusted OR (95% CI)	β	P
age	1.093 [1.060-1.127]	0.089	< 0.001
PSA	1.086 [1.042-1.132]	0.083	< 0.001
f/t PSA	2.106 [1.225-3.622]	0.745	0.007
PSAD	3.784 [2.041-7.015]	1.331	< 0.001
PV	0.962 [0.947-0.977]	-0.039	< 0.001
DRE	1.389 [0.675-2.856]	0.328	0.372

(P < 0.001). The median lesion size was 7.5 mm (IQR, 6-11) in the csPCa group versus 7 mm (IQR, 5-11) in the indolent PCa group with lesion quantities averaging 1.26 and 1.12, respectively. Univariate regression analysis identified age, PSA, f/t PSA, PSAD, DRE, and PV as significant csPCa predictors (P < 0.05, **Table 1**). Multivariate logistic regression analysis highlighted age (OR=1.093, [95% CI: 1.060-1.127], P < 0.001), PSA (OR=1.086, [95% CI: 1.042-1.132], P < 0.001), f/t PSA (OR=2.106, [95% CI: 1.225-3.622], P=0.007), PV (OR=0.962, [95% CI: 0.947-0.977], P < 0.001), PSAD (OR=3.784, [95% CI: 2.041-7.015], P < 0.001) were the risk factors of csPCa. In contrast, the variable DRE did not show a statistically significant difference (OR=1.389, [95% CI: 0.675-2.856], P=0.372) (**Table 2**).

Nomogram for PZ

As for the PZ patient group, detection rates for PCa and csPCa were 58.4% and 44.8%, respectively. Univariate logistic regression identified age, PSA, PV, and PSAD as significant predictors for csPCa. The Multivariate analysis also underscored the significance of age (OR=1.100, [95% CI: 1.050-1.153], P < 0.001), PSA (OR=1.113, [95% CI: 1.020-1.215], P= 0.016), and PV (OR=0.951, [95% CI: 0.925-0.977], P < 0.001) as risk factors for the diagnosis of csPCa on initial biopsy. A nomogram incorporating each of these clinical variables is shown in **Figure 2A**. The ROC was then generated, and the AUC value of the model was 0.819 (95% CI: 0.769-0.868) (**Figure 3**). The calibration plot shown in **Figure 4** demonstrated high degree of agreements with clinical finding. DCA also showed that the prediction model achieved an optimal overall net benefit. Within the threshold risk range of 10% to 75%, intervention decisions based on the predictive model are beneficial (**Figure 5**).

Nomogram for TZ

Among the 245 TZ patients, 30.6% (75/245) were diagnosed with PCa, while only 18.4% (45/245) were diagnosed with csPCa. Significant predictors of csPCa included age, f/t PSA, PV, and PSAD. Multivariate analysis revealed that age (OR=1.075, [95% CI: 1.025-1.120], P=0.003), f/t PSA (OR=0.002, [95% CI: 0.000-0.532], P=0.029), PSAD (OR=0.956, [95% CI: 0.927-0.958], P=0.003) were notable risk factors of csPCa (P < 0.05). A nomogram was generated in line with the final logistic regression model to assess the risk of being diagnosed with csPCa outcome with an AUC of

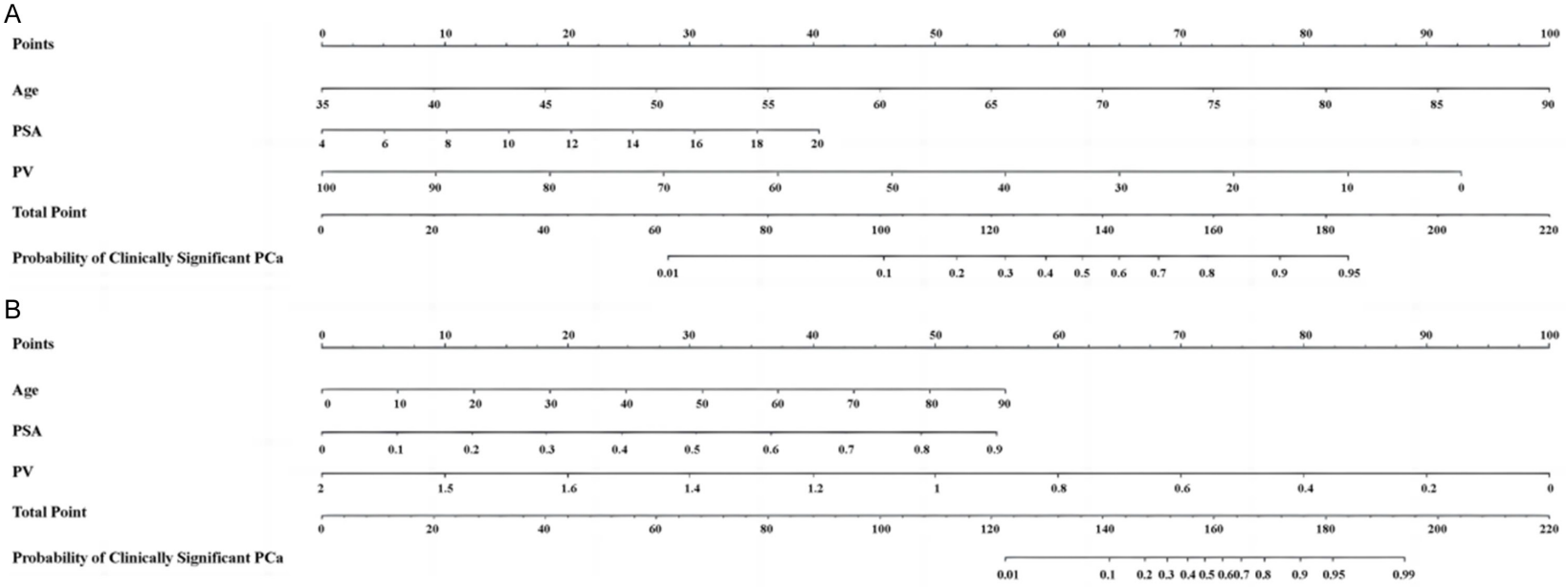

Figure 2. Nomogram to predict the probability of clinically significant prostate cancer. A. Nomogram to predict the probability of clinically significant prostate cancer peripheral zone group. B. Nomogram to predict the probability of clinically significant prostate cancer transitional zone group.

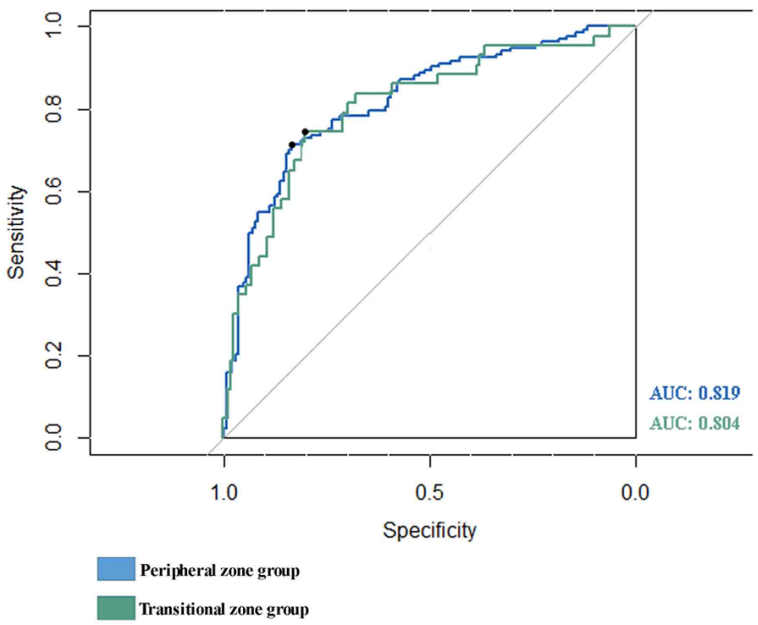

Figure 3. The area under the receiver operating characteristic curve of the prediction model for peripheral zone and transitional zone group.

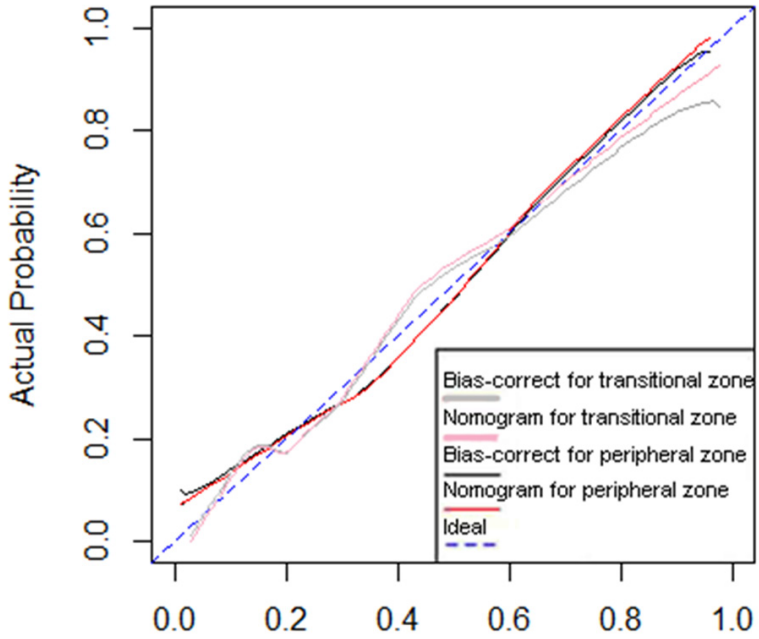

Figure 4. The calibration curve of the nomograms for peripheral zone and transitional zone group.

0.804 (95% CI: 0.726-0.881) (**Figures 2B**, **3**). Calibration plot of predicted probability of csPCa is shown in **Figure 4** and elucidated excellent predictive accuracy. DCA also showed superior benefit across most threshold ranges (15%-80%) (**Figure 5**).

External validation of a nomogram

External validation was conducted on an independent cohort of 238 patients, with 72 cases of csPCa identified. Supplementary Table 3 demonstrates the baseline characteristics of the external cohort. No significant difference was detected between the external validation group and the training group (Supplementary Table 4). In external validation, the AUCs for PZ and TZ were 0.831 (95% CI: 0.747-0.914) and 0.773 (95% CI: 0.725-0.882), respectively, demonstrating consistency after 1000 bootstrap resamples (**Figure 6**). The DeLong test confirmed no significant AUC differences between training and validation nomograms (P=0.987 for PZ; P=0.889 for TZ). The Hosmer-Lemeshow test *p*-value indicated a proper fit for both PZ (χ^2=6.30, P=0.608) and TZ (χ^2=4.28, P=0.830). According to the DCA, the nomograms also showed high clinical applicability in the external cohort (the maximum threshold probability was 0.50 in the PZ group and 0.63 in the TZ group) (**Figure 7**).

In the ROC analysis, the AUC for each single variable was 0.667 (age), 0.681 (PSA), 0.664 (f/t PSA), 0.681 (PSAD), 0.693 (PV) and 0.642 (DRE) (**Figure 8**). The results indicated that the combined nomograms significantly outperform each variable alone, with AUCs of 0.819 for PZ and 0.804 for TZ, both P < 0.001. Compared with performing biopsy for patients with PI-RADS 3 lesions based on traditional mpMRI with DCE, utilizing our nomograms could increase the csPCa detection rate from 42.4% to 53.6% for PZ and

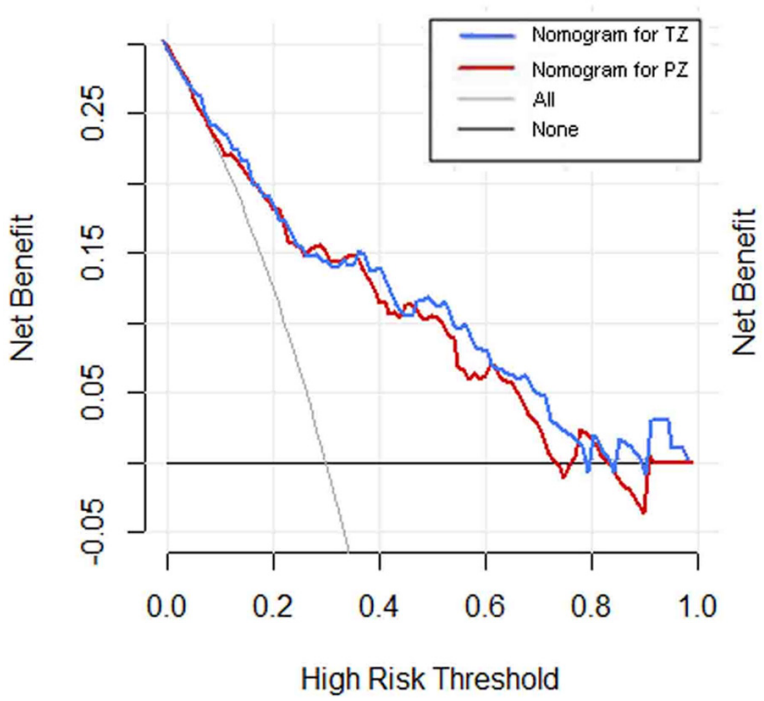

Figure 5. Decision curve for predicting clinically significant prostate cancer for peripheral zone and transitional zone group.

17.0% to 25.3% for TZ, while reducing unnecessary biopsies by 27.3% for PZ and 51.2% for TZ, with minimal missed csPCa cases (9.3% for PZ and 7.4% for TZ).

Discussion

Currently, mpMRI has undoubtedly gained momentum as a diagnostic tool to detect PCa and is currently considered as the optimal imaging diagnostic tool for evaluating primary PCa. In biopsy-naïve men, a crucial goal is minimizing overdiagnosis while ensuring csPCa is detected. Current strategies for PI-RADS 1, 2, 4, and 5 lesions are well-established in previous research; however, the management of PI-RADS 3 lesions remains debatable [20]. Therefore, identifying and standardizing the most effective clinical data for these lesions is a pressing need. Recent studies have developed several nomograms based on bpMRI or mpMRI and demonstrated similar results with AUC ranged from 0.81-0.93 [21-25]. Niu et al. developed a prediction model based on bpMRI incorporating age and PSAD, and this model showed 87.3% sensitivity and 78.4% specificity for diagnosing csPCa but lacks external validation and requires to be tested and verified in more centers with larger samples [26]. The bpMRI-based nomograms developed by Lee et al. achieved a 92% diagnostic rate for csPCa, but nearly 20% of these patients underwent repeat biopsies, which may lead to a misestimate of the diagnostic accuracy of the model [27]. According to our results, the final nomograms achieved an AUC of 0.819 for PZ and 0.804 for TZ, which can be translated into a practicable predictive model with eligible calibration. In addition, our study also demonstrates that PI-RADS 3 lesions are more prevalent in the TZ than in the PZ, and the detection rate of csPCa is significantly lower in TZ than in PZ. Given that the lesions in different zones has significantly different csPCa detection rates, we analyzed and eventually explored nomograms with bpMRI and clinical information for the prediction of csPCa according to the different prostate zones; among the 21 csPCa patients with DCE-upgraded category 3 lesions, 20 of them could be perfectly identified by our nomograms. Our model was additionally tested on a significantly different external test cohort and retained an AUC of 0.831 for PZ and 0.773 for TZ with high accuracy and calibration agreement. The majority of the previous demonstrated studies lacked external validation with limited sample sizes whereas in the present study, external validation was used to make our model more convincing.

Under the PI-RADS v2.1 guidelines, DCE sequences play a critical role in staging PCa, particularly in grading PI-RADS 3 lesions within the PZ. The application of DCE as an integral part of mpMRI in addition to T2WI and DWI has been discussed controversially in recent literature [28]. Scialpi et al. highlighted that the DCE application could significantly improve the detection of small lesions (< 7 mm), which would probably be ignored with bpMRI alone [29]. Without DCE imaging, this is particularly true for subtle tumors in the PZ, where their small size, poor contrast, proximity to benign

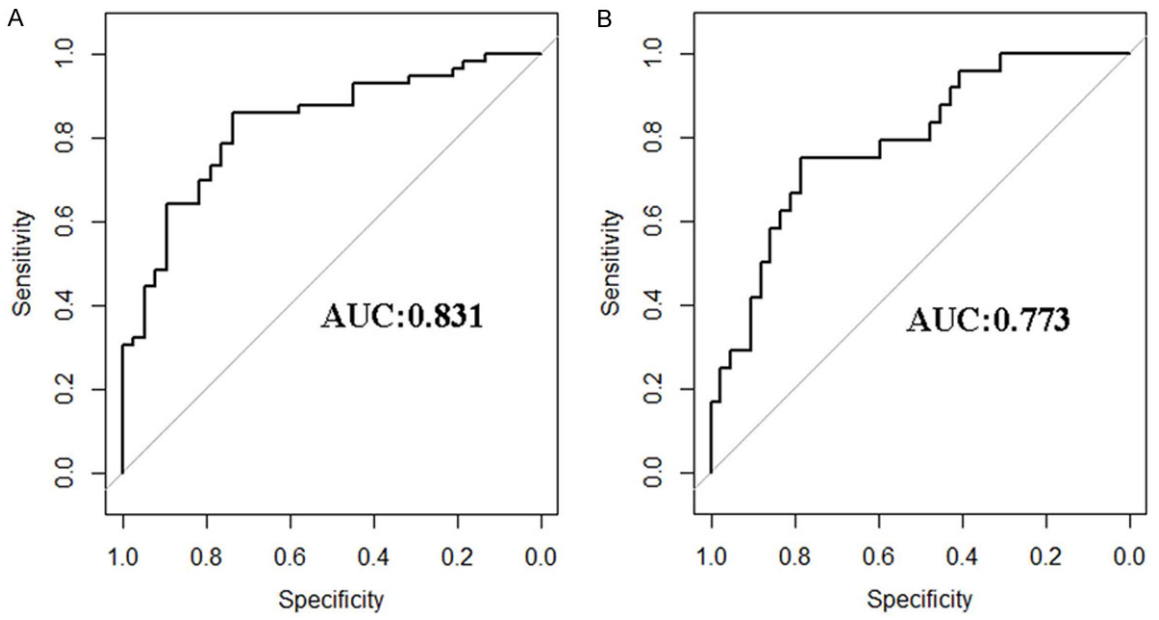

Figure 6. The area under the receiver operating characteristic curve of the prediction model for external validation. A. The area under the receiver operating characteristic curve of the prediction model for peripheral zone group. B. The area under the receiver operating characteristic curve of the prediction model for transitional zone group.

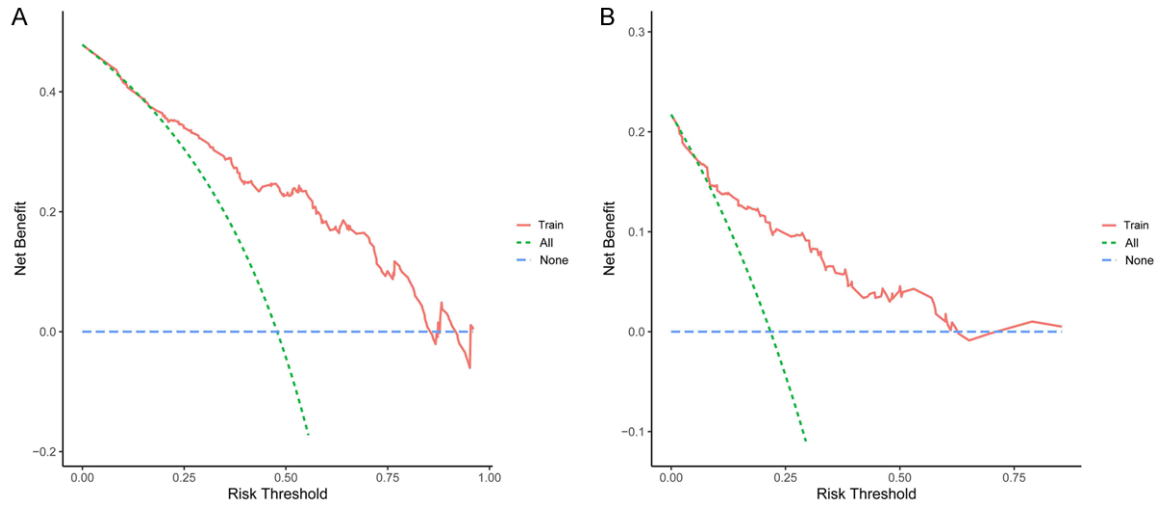

Figure 7. Decision curve analysis of the nomogram in external validation set. A. Decision curve analysis of the nomogram for the peripheral zone. B. Decision curve analysis of the nomogram for the transitional zone.

tissue, or challenging location within the prostate, can lead to missed diagnoses using only T2WI and DWI. According to Wei et al., the inter-reader agreement through the PI-RADS v2.1 protocol was substantial (kappa value of 0.648) for TZ lesions [23]. Greer et al. indicated that PI-RADS category 3 lesions at DWI with positive at DCE in the PZ demonstrated a higher probability of cancer than DCE-negative PI-RADS category 3 lesions (67.8% *vs.* 40.0%, P=0.02) [30]. According to a literature review by Geer et al., covering 2014-2017, the prevalence of clinically csPCa in PI-RADS 3 patients was approximately 21% (4-27%) based on index lesions [31].

To sum up, our study introduces novel nomograms that may partially substitute the DCE sequence. To the best of our knowledge, this is the first study that demonstrated the potential

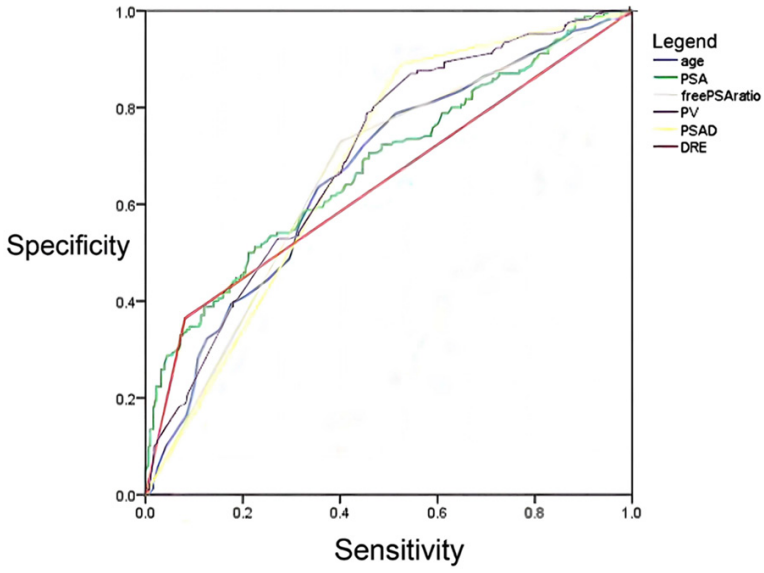

Figure 8. The area under the receiver operating characteristic curve for the included variables.

utility of nomograms with analysis of bpMRI for identification of csPCa in PI-RADS 3 patients with PSA lelvels of 4-20 ng/mL. Distinguishing our approach, we focus more on the indeterminate probability of malignancy zone, which could significantly strengthen the applicability and benefits of the model in clinical practices. Multiple previous studies have demonstrated that PSAD plays a positive role in the combined diagnosis of PCa or csPCa [32, 33]. Considering the total level of PSA and PV, PSAD is more individualized significance than total PSA, as previously proved in the literature. Our study also confirms PSAD's added value in diagnosing csPCa in the TZ. In addition, it is commonly accepted that benign prostatic hyperplasia (BPH) lesions are mostly located in the TZ while PCa usually occurs in the PZ of the prostate. The fPSA is the fraction of tPSA that does not bind in serum, its concentration is lower in malignancy patients than in BPH patients, thus f/t PSA is more valuable for clinical application when a lesion located at TZ [34]. In our study, f/t PSA was included in the nomogram for PZ as a significant variable for the prediction of csPCa, which met the results of the former study [35].

Our study has several limitations that need to be reported. First, although we performed a set of inclusive and exclusive criteria during the data collection, bias could not be completely avoided. Such as the protocol of biopsy and mpMRI interpretation by different clinicians, inter-institutional outcomes could not be well evaded. Such factors are inevitable in clinical practice because each hospital is independent. Although the heterogeneity existed in the two centers, our model was still stable during construction and validation, which suggests that our model has high generalizability. Nevertheless, our results still need to be validated by a large-scale prospective multicenter study. Second, PI-RADS 3 datasets were too small and imbalanced to generalize results. In addition, the standard of reference was achieved by cognitive fusion biopsy, as per the description. For the majority of cases, fusion biopsy sufficient, however, for large prostate with a PI-RADS 3 lesions in the middle of the TZ, cognitive fusion biopsy may be challenging. A larger and more balanced study group is needed to build more promising prediction models. Third, we also noticed that other advanced imaging modalities available - such as 68Ga prostate-specific membrane antigen scanning and 18-F fluorocyclobutane-1-carboxylic acid PET/CT [36, 37] were not incorporated in the present study. Updating available models (for example: the ERSPC calculator) or building new multivariable predictors to include novel indicators such as PCA3 could provide further benefit [38, 39]. Moreover, in the future, our team will continue our research to provide new methods for nomograms incorporating bpMRI characteristics such as MRI radiomics for csPCa diagnosis.

Conclusion

In this study, we have successfully established and validated nomograms for predicting the probability of csPCa in initial prostate biopsy based on six easily obtained factors, including age, PSA, DRE, f/t PSA, PV, and PSAD. These factors are novel risk calculators for patients with an indeterminate probability of malignancy according to bpMRI and a total PSA between

4-20 ng/mL. The nomograms created in this study can be further applied to guide clinical decision-making. Future studies should aim to validate these nomograms through a larger population.

Disclosure of conflict of interest

None.

Address correspondence to: Zhien Zhou and Weigang Yan, Department of Urology, Surgical Building of Peking Union Medical College Hospital, Peking Union Medical College, Chinese Academy of Medical Sciences, No. 1 Shuaifuyuan, Wangfujing, Dong Cheng District, Beijing 100730, China. E-mail: zhouzhien@pumch.cn (ZEZ); yanweigang@pumch.cn (WGY); Fenghong Cao, Department of Urology, North China University of Science and Technology Affiliated Hospital, No. 73 Jianshe South Road, Tangshan 063000, Hebei, China. E-mail: caofenghong@ncst.edu.cn

References

[1] Siegel RL, Miller KD, Fuchs HE and Jemal A. Cancer statistics, 2022. CA Cancer J Clin 2022; 72: 7-33.

[2] Sung H, Ferlay J, Siegel RL, Laversanne M, Soerjomataram I, Jemal A and Bray F. Global cancer statistics 2020: GLOBOCAN estimates of incidence and mortality worldwide for 36 cancers in 185 countries. CA Cancer J Clin 2021; 71: 209-249.

[3] Bill-Axelson A, Holmberg L, Garmo H, Taari K, Busch C, Nordling S, Häggman M, Andersson SO, Andrén O, Steineck G, Adami HO and Johansson JE. Radical prostatectomy or watchful waiting in prostate cancer - 29-year follow-up. N Engl J Med 2018; 379: 2319-2329.

[4] Welch HG and Albertsen PC. Reconsidering prostate cancer mortality - the future of PSA screening. N Engl J Med 2020; 382: 1557-1563.

[5] Ziglioli F, Granelli G, Cavalieri D, Bocchialini T and Maestroni U. What chance do we have to decrease prostate cancer overdiagnosis and overtreatment? A narrative review. Acta Biomed 2019; 90: 423-426.

[6] Patel P, Wang S and Siddiqui MM. The use of multiparametric magnetic resonance imaging (mpMRI) in the detection, evaluation, and surveillance of clinically significant prostate cancer (csPCa). Curr Urol Rep 2019; 20: 60.

[7] Kuhl CK, Bruhn R, Krämer N, Nebelung S, Heidenreich A and Schrading S. Abbreviated biparametric prostate MR imaging in men with elevated prostate-specific antigen. Radiology 2017; 285: 493-505.

[8] Jambor I, Boström PJ, Taimen P, Syvänen K, Kähkönen E, Kallajoki M, Perez IM, Kauko T, Matomäki J, Ettala O, Merisaari H, Kiviniemi A, Dean PB and Aronen HJ. Novel biparametric MRI and targeted biopsy improves risk stratification in men with a clinical suspicion of prostate cancer (IMPROD Trial). J Magn Reson Imaging 2017; 46: 1089-1095.

[9] Boesen L, Nørgaard N, Løgager V, Balslev I, Bisbjerg R, Thestrup KC, Winther MD, Jakobsen H and Thomsen HS. Assessment of the diagnostic accuracy of biparametric magnetic resonance imaging for prostate cancer in biopsy-naive men: the biparametric MRI for detection of prostate cancer (BIDOC) study. JAMA Netw Open 2018; 1: e180219.

[10] Porter KK, King A, Galgano SJ, Sherrer RL, Gordetsky JB and Rais-Bahrami S. Financial implications of biparametric prostate MRI. Prostate Cancer Prostatic Dis 2020; 23: 88-93.

[11] Yilmaz EC, Shih JH, Belue MJ, Harmon SA, Phelps TE, Garcia C, Hazen LA, Toubaji A, Merino MJ, Gurram S, Choyke PL, Wood BJ, Pinto PA and Turkbey B. Prospective evaluation of PI-RADS version 2.1 for prostate cancer detection and investigation of multiparametric MRI-derived markers. Radiology 2023; 307: e221309.

[12] Messina E, Pecoraro M, Laschena L, Bicchetti M, Proietti F, Ciardi A, Leonardo C, Sciarra A, Girometti R, Catalano C and Panebianco V. Low cancer yield in PI-RADS 3 upgraded to 4 by dynamic contrast-enhanced MRI: is it time to reconsider scoring categorization? Eur Radiol 2023; 33: 5828-5839.

[13] Perez IM, Jambor I, Kauko T, Verho J, Ettala O, Falagario U, Merisaari H, Kiviniemi A, Taimen P, Syvänen KT, Knaapila J, Seppänen M, Rannikko A, Riikonen J, Kallajoki M, Mirtti T, Lamminen T, Saunavaara J, Pahikkala T, Boström PJ and Aronen HJ. Qualitative and quantitative reporting of a unique biparametric MRI: towards Biparametric MRI-Based nomograms for prediction of prostate biopsy outcome in men with a clinical suspicion of prostate cancer (IMPROD and MULTI-IMPROD trials). J Magn Reson Imaging 2020; 51: 1556-1567.

[14] Jambor I, Verho J, Ettala O, Knaapila J, Taimen P, Syvänen KT, Kiviniemi A, Kähkönen E, Perez IM, Seppänen M, Rannikko A, Oksanen O, Riikonen J, Vimpeli SM, Kauko T, Merisaari H, Kallajoki M, Mirtti T, Lamminen T, Saunavaara J, Aronen HJ and Boström PJ. Validation of IMPROD biparametric MRI in men with clinically suspected prostate cancer: a prospective multi-institutional trial. PLoS Med 2019; 16: e1002813.

[15] Snell KIE, Levis B, Damen JAA, Dhiman P, Debray TPA, Hooft L, Reitsma JB, Moons KGM, Collins GS and Riley RD. Transparent reporting of multivariable prediction models for individual prognosis or diagnosis: checklist for systematic reviews and meta-analyses (TRIPOD-SRMA). BMJ 2023; 381: e073538.

[16] Casagrande A, Fabris F and Girometti R. Beyond kappa: an informational index for diagnostic agreement in dichotomous and multivalue ordered-categorical ratings. Med Biol Eng Comput 2020; 58: 3089-3099.

[17] Kuru TH, Wadhwa K, Chang RT, Echeverria LM, Roethke M, Polson A, Rottenberg G, Koo B, Lawrence EM, Seidenader J, Gnanapragasam V, Axell R, Roth W, Warren A, Doble A, Muir G, Popert R, Schlemmer HP, Hadaschik BA and Kastner C. Definitions of terms, processes and a minimum dataset for transperineal prostate biopsies: a standardization approach of the Ginsburg Study Group for Enhanced Prostate Diagnostics. BJU Int 2013; 112: 568-577.

[18] Epstein JI, Walsh PC, Carmichael M and Brendler CB. Pathologic and clinical findings to predict tumor extent of nonpalpable (stage T1c) prostate cancer. JAMA 1994; 271: 368-374.

[19] Vickers AJ and Elkin EB. Decision curve analysis: a novel method for evaluating prediction models. Med Decis Making 2006; 26: 565-574.

[20] Hansen NL, Barrett T, Koo B, Doble A, Gnanapragasam V, Warren A, Kastner C and Bratt O. The influence of prostate-specific antigen density on positive and negative predictive values of multiparametric magnetic resonance imaging to detect Gleason score 7-10 prostate cancer in a repeat biopsy setting. BJU Int 2017; 119: 724-730.

[21] Alberts AR, Roobol MJ, Verbeek JFM, Schoots IG, Chiu PK, Osses DF, Tijsterman JD, Beerlage HP, Mannaerts CK, Schimmöller L, Albers P and Arsov C. Prediction of high-grade prostate cancer following multiparametric magnetic resonance imaging: improving the rotterdam European randomized study of screening for prostate cancer risk calculators. Eur Urol 2019; 75: 310-318.

[22] Meyerson BL, Streicher J and Sidana A. A magnetic resonance imaging-based prediction model for prostate biopsy risk stratification. Ther Adv Urol 2018; 10: 357-358.

[23] Wei C, Pan P, Chen T, Zhang Y, Dai G, Tu J, Jiang Z, Zhao W and Shen J. A nomogram based on PI-RADS v2.1 and clinical indicators for predicting clinically significant prostate cancer in the transition zone. Transl Androl Urol 2021; 10: 2435-2446.

[24] Pan JF, Su R, Cao JZ, Zhao ZY, Ren DW, Ye SZ, Huang RD, Tao ZL, Yu CL, Jiang JH and Ma Q. Modified predictive model and nomogram by incorporating prebiopsy biparametric magnetic resonance imaging with clinical indicators for prostate biopsy decision making. Front Oncol 2021; 11: 740868.

[25] Zhou ZH, Liu F, Wang WJ, Liu X, Sun LJ, Zhu Y, Ye DW and Zhang GM. Development and validation of a nomogram including lymphocyte-to-monocyte ratio for initial prostate biopsy: a double-center retrospective study. Asian J Androl 2021; 23: 41-46.

[26] Niu XK, Li J, Das SK, Xiong Y, Yang CB and Peng T. Developing a nomogram based on multiparametric magnetic resonance imaging for forecasting high-grade prostate cancer to reduce unnecessary biopsies within the prostate-specific antigen gray zone. BMC Med Imaging 2017; 17: 11.

[27] Lee SM, Liyanage SH, Wulaningsih W, Wolfe K, Carr T, Younis C, Van Hemelrijck M, Popert R and Acher P. Toward an MRI-based nomogram for the prediction of transperineal prostate biopsy outcome: a physician and patient decision tool. Urol Oncol 2017; 35: 664.e611-664.e618.

[28] Kang Z, Min X, Weinreb J, Li Q, Feng Z and Wang L. Abbreviated biparametric versus standard multiparametric MRI for diagnosis of prostate cancer: a systematic review and meta-analysis. AJR Am J Roentgenol 2019; 212: 357-365.

[29] Scialpi M, Prosperi E, D'Andrea A, Martorana E, Malaspina C, Palumbo B, Orlandi A, Falcone G, Milizia M, Mearini L, Aisa MC, Scialpi P, DE Dominicis C, Bianchi G and Sidoni A. Biparametric versus multiparametric MRI with non-endorectal coil at 3T in the detection and localization of prostate cancer. Anticancer Res 2017; 37: 1263-1271.

[30] Greer MD, Shih JH, Lay N, Barrett T, Kayat Bittencourt L, Borofsky S, Kabakus IM, Law YM, Marko J, Shebel H, Mertan FV, Merino MJ, Wood BJ, Pinto PA, Summers RM, Choyke PL and Turkbey B. Validation of the dominant sequence paradigm and role of dynamic contrast-enhanced imaging in PI-RADS version 2. Radiology 2017; 285: 859-869.

[31] Greer MD, Shih JH, Lay N, Barrett T, Kayat Bittencourt L, Borofsky S, Kabakus IM, Law YM, Marko J, Shebel H, Mertan FV, Merino MJ, Wood BJ, Pinto PA, Summers RM, Choyke PL and Turkbey B. Validation of the dominant sequence paradigm and role of dynamic contrast-enhanced imaging in PI-RADS version 2. Radiology 2017; 285: 859-869.

[32] Han C, Liu S, Qin XB, Ma S, Zhu LN and Wang XY. MRI combined with PSA density in detect-

ing clinically significant prostate cancer in patients with PSA serum levels of 4~10 ng/mL: biparametric versus multiparametric MRI. Diagn Interv Imaging 2020; 101: 235-244.
[33] Lee SJ, Oh YT, Jung DC, Cho NH, Choi YD and Park SY. Combined analysis of biparametric MRI and prostate-specific antigen density: role in the prebiopsy diagnosis of gleason score 7 or greater prostate cancer. AJR Am J Roentgenol 2018; 211: W166-W172.
[34] Huang Y, Li ZZ, Huang YL, Song HJ and Wang YJ. Value of free/total prostate-specific antigen (f/t PSA) ratios for prostate cancer detection in patients with total serum prostate-specific antigen between 4 and 10ng/mL: a meta-analysis. Medicine (Baltimore) 2018; 97: e0249.
[35] Bachour DM, Chahin E and Al-Fahoum S. Human kallikrein-2, prostate specific antigen and free- prostate specific antigen in combination to discriminate prostate cancer from benign diseases in syrian patients. Asian Pac J Cancer Prev 2015; 16: 7085-7088.
[36] Alongi P, Laudicella R, Lanzafame H, Farolfi A, Mapelli P, Picchio M, Burger IA, Iagaru A, Minutoli F and Evangelista L. PSMA and choline PET for the assessment of response to therapy and survival outcomes in prostate cancer patients: a systematic review from the literature. Cancers (Basel) 2022; 14: 1170.
[37] Evangelista L, Briganti A, Fanti S, Joniau S, Reske S, Schiavina R, Stief C, Thalmann GN and Picchio M. New clinical indications for (18) F/(11)C-choline, new tracers for positron emission tomography and a promising hybrid device for prostate cancer staging: a systematic review of the literature. Eur Urol 2016; 70: 161-175.
[38] Jiang Z, Zhao Y and Tian Y. Comparison of diagnostic efficacy by two urine PCA3 scores in prostate cancer patients undergoing repeat biopsies. Minerva Urol Nefrol 2019; 71: 373-380.
[39] Merola R, Tomao L, Antenucci A, Sperduti I, Sentinelli S, Masi S, Mandoj C, Orlandi G, Papalia R, Guaglianone S, Costantini M, Cusumano G, Cigliana G, Ascenzi P, Gallucci M and Conti L. PCA3 in prostate cancer and tumor aggressiveness detection on 407 high-risk patients: a National Cancer Institute experience. J Exp Clin Cancer Res 2015; 34: 15.

Supplementary Table 1. PI-RADS scoring criteria

PZ			TZ		
DWI	T2WI	PI-RADS	T2WI	DWI	PI-RADS
1	any	1	1	any	1
2	any	2	2	any	2
3	any	3	3	≤ 4	3
				5	4
4	any	4	4	any	4
5	any	5	5	any	5

Supplementary Table 2. Prostate biparametric magnetic resonance imaging protocol

Parameters	T2WI	DWI
Sequence	FRFSE	SE-EPI
TR/TE (ms)	4200/90	4200/90
Flip angle (degree)	110	90
Echo train length	32	1
Field of view (mm × mm)	270 × 270	360 × 360
Matrix size	288 × 192	128 × 96
Thickness (mm)	3.0	3.0
Other		b values = 0, 800, 1000, mm^2/sec

T2WI, T2-weighted imaging; DWI, diffusion-weighted imaging; TR, repetition time; TE, time echo; FRFSE, fast relaxation fast spin echo; SE-EPI, spin-echo echo planar imaging; 3D-GRE, 3D-gradient echo.

Supplementary Table 3. Baseline characteristics of included patients for external validation

Variables	insPCa		csPCa	P
	Non-PCa	indolent PCa		
Patients n	135	31	72	
Age (median)	64 (59-69)	64 (62-76)	70 (65-77)	< 0.001
PSA (median)	8.30 (5.98-10.77)	6.81 (5.84-10.20)	9.20 (5.98-14.65)	< 0.001
f/t PSA (median)	0.147 (0.104-0.208)	0.157 (0.115-0.199)	0.097 (0.073-0.175)	< 0.001
PV (median)	50 (35-65)	35 (26-50)	35 (30-47)	< 0.001
PSAD (median)	0.173 (0.103-0.248)	0.198 (0.154-0.320)	0.286 (0.180-0.404)	< 0.001

Supplementary Table 4. The comparison of baseline characteristics between training group and external validation group

	Training group (n=457)	Validation group (n=238)	*P* value
Age (median, IQR)	65 (61-71)	64 (59-68)	0.959
PSA (median, IQR)	8.01 (6.23-10.92)	8.35 (5.98-10.77)	0.457
PSAD (median, IQR)	0.184 (0.122-0.263)	0.173 (0.103-0.248)	0.631
f/t PSA (median, IQR)	0.151 (0.104-0.234)	0.147 (0.104-0.208)	0.821
PV (median, IQR)	45 (35-60)	50 (35-65)	0.194
csPCa (n)	140	72	0.338